**Title: A Versatile Remediation Module for Remote Repair of Spent Nuclear Fuel and High-Level Waste Storage Containers**

**Authors:**

Stylianos Chatzidakis,[1,*] Dominic Giuliano,[2] Jeremy Slade,[2] Wei Tang,[3] Roger Miller,[3] Steve Reeves,[4] John Scaglione,[1] and Robert Howard[1]

[1]Reactor and Nuclear Systems Division, Oak Ridge National Laboratory, Oak Ridge, TN 37831

[2]Fusion Energy Division, Oak Ridge National Laboratory, Oak Ridge, TN 37831

[3]Materials Science and Technology Division, Oak Ridge National Laboratory, Oak Ridge, TN 37831

[4]US Department of Energy, Germantown, MD 20874

[*]**Contact Info:**

Tel: +1 865-576-8981, Email: chatzidakiss@ornl.gov, ORCID: 0000-0003-1268-000X

**Abstract:**

*Oak Ridge National Laboratory (ORNL) successfully demonstrated the Versatile Remediation Module (VRM), a prototype module designed and built by ORNL for on-site remote repair of welded stainless-steel storage containers for spent nuclear fuel and high-level radioactive waste. This paper describes the VRM prototype and its design features and components to support continued long-term storage or off-site transportation of spent nuclear fuel and high-level radioactive waste currently stored in storage containers. A remote (100 ft away from the simulated radiative environment) demonstration of the VRM was successfully performed on a full-scale mockup welded stainless steel canister. The VRM is designed with features to accommodate remediation techniques beyond those currently selected and described in this paper. Therefore, many of the VRM's features may benefit other remote nuclear or nonnuclear applications. The VRM is envisioned to serve as a development center to facilitate and enhance further development of new remediation technologies.*

Keywords: spent nuclear fuel, remote repair, remediation, arc welding

*This manuscript has been authored by UT-Battelle, LLC, under contract DE-AC05-00OR22725 with the US Department of Energy (DOE). The US government retains and the publisher, by accepting the article for publication, acknowledges that the US government retains a nonexclusive, paid-up, irrevocable, worldwide license to publish or reproduce the published form of this manuscript, or allow others to do so, for US government purposes. DOE will provide public access to these results of federally sponsored research in accordance with the DOE Public Access Plan (http://energy.gov/downloads/doe-public-access-plan).*

## I. Introduction

The continued storage and off-site transportation of spent nuclear fuel currently stored in dry storage systems (DSSs) could be affected by aging of the confinement boundary and by the impact of aging on system performance (Fig. 1) [1–7]. Hence, efforts to support development of remediation capabilities that could be used at multiple storage installations have been identified as a priority need [8]. These capabilities would permit repairs to existing DSSs for continued storage or off-site transportation, if necessary. Previous work [9] identified and evaluated mitigation and remediation methods and techniques for welded stainless-steel canisters and their components as part of the confinement boundary. Chatzidakis et al. concluded that five options are available: (1) use as is, (2) overpack, (3) repair, (4) rework, and (5) replace (i.e., repackage).

Since 2019, efforts have been underway to develop remediation capabilities for remote remediation of a DSS, if needed. In support of this effort, Oak Ridge National Laboratory (ORNL) is developing a Mobile Examination and Remediation Fixture (MERF) with functions and capabilities for onsite remediation of nonconforming canisters/casks [10]. Once developed, the MERF (shown schematically in Fig. 2) would be intended to perform necessary processes to ascertain the condition of dry storage canisters and perform repairs when necessary. Specifically, the MERF would be functionally designed to inspect a canister using various nondestructive examination (NDE) methods, excavate material surrounding identified flaws, and perform repair welds on the affected area of the canister. To achieve a complete remediation, the MERF is anticipated to have at least three modules: the weld repair module, the NDE module, and the surface preparation module. The MERF would comprise tool modules to allow for remote remediation operations (e.g., inspecting, welding, grinding) on the canister's surface. The canister would be placed on a rotary table for coarse positioning to allow for rotation of the canister in clockwise and counterclockwise directions. The modules would be placed on a lifting platform and positioned in front of the remediation area. The modules and the canister would be surrounded by shielding to protect operating personnel from radiation exposure, and the MERF would accommodate canisters with nominal diameters in the range of 1701.8 to 1917.7 mm (67 to 75.5 in.). ORNL successfully built and demonstrated the first module, hereafter referred to as the Versatile Remediation Module (VRM), which focuses on weld repair. Future development will include additional modules, i.e., NDE and surface preparation, to performe functions needed for a complete canister remediation.

Radiation levels at the surface of storage containers preclude any personnel access during remediation operations. Therefore, remediation operations must be performed remotely, for example within a shielded facility, e.g., hot cell, or using a MERF type concept.. Additionally, operations should be largely automated to meet quality and time requirements. This paper describes the design, features, and components of the VRM that enable remote and automated delivery of remediation tools to any point on a spent nuclear fuel canister's cylindrical wall. This paper also presents procedure qualification results, an operational sequence, and the results of a remote (30 m away from the simulated radiative environment) demonstration of the VRM on a full-scale mockup welded stainless steel canister.

Remediation of storage containers is an active development area, and advanced remediation technologies might become available soon. Therefore, the VRM was designed with features to accommodate remediation techniques beyond those currently selected and described in this paper. Also, the VRM is designed with enough flexibility to be used either within a shielded facility or as part of the MERF concept. The VRM could serve as a development center to facilitate and enhance further development of new remediation technologies. Furthermore, many VRM features may benefit other remote nuclear or nonnuclear applications.

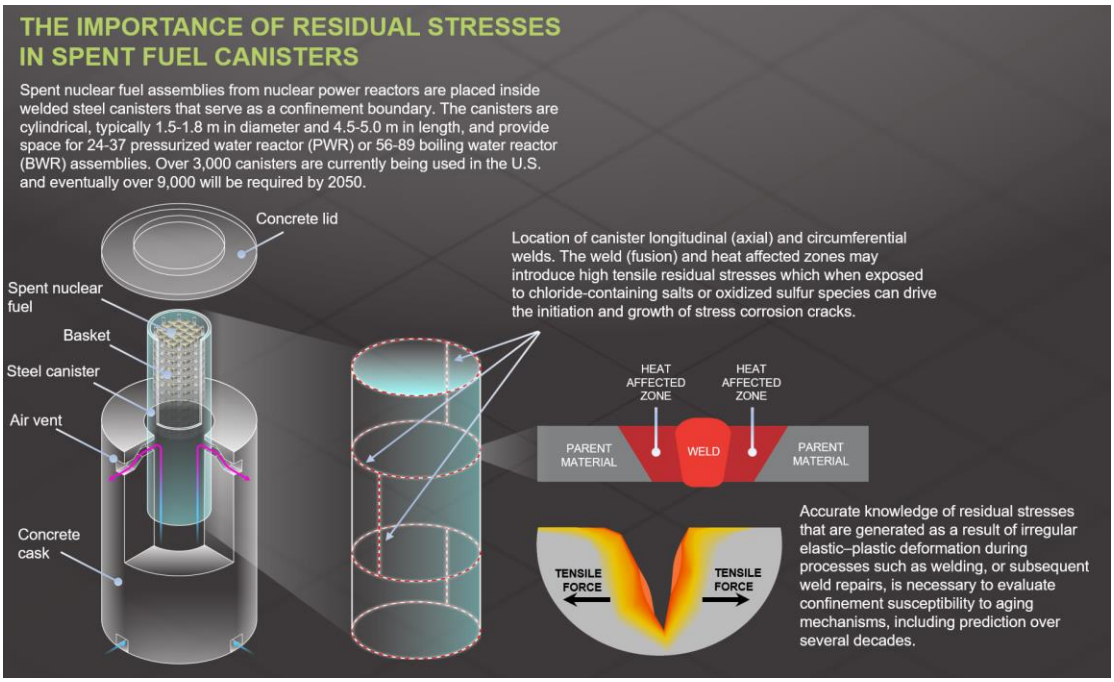


**Figure 1. Illustration of a vertical spent nuclear fuel dry storage system (DSS).** The vertical DSS comprises a concrete overpack to provide structural support and radiation shielding, and a welded steel canister to serve as a confinement boundary for spent nuclear fuel. Approximately 90% of dry storage systems are based on welded stainless-steel canisters placed in concrete overpacks, and 65% of all the canisters are vertically oriented [11]. The potential for stress corrosion cracking at the heat affected zones of welded stainless steel interim storage canisters for spent nuclear fuel has been identified as a high priority data gap by several agencies [12–16].

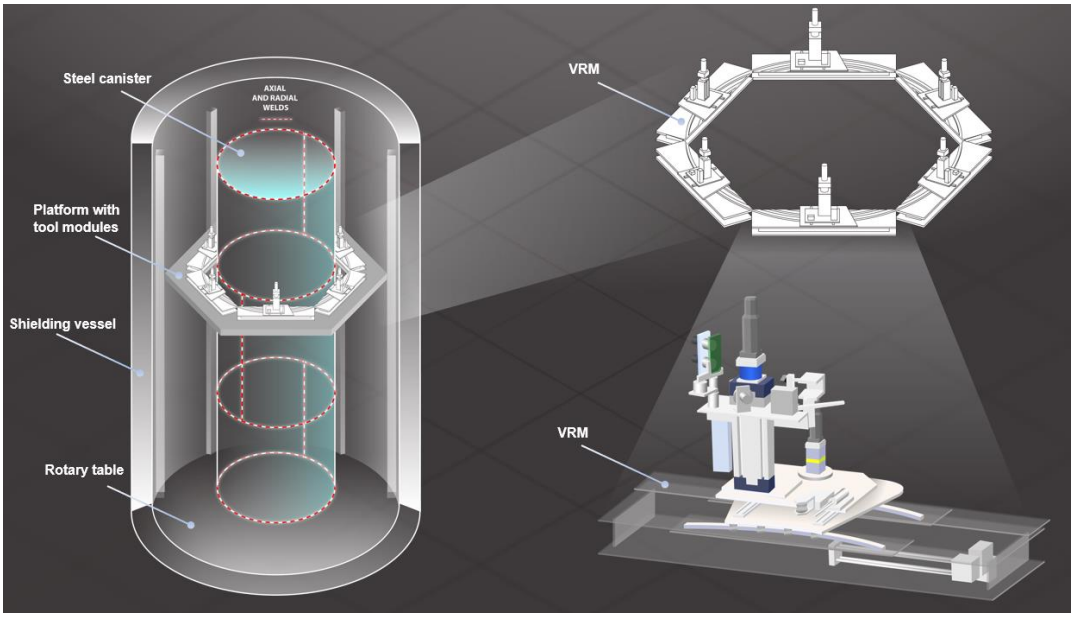


**Figure 2. Mobile Examination and Remediation Fixture (MERF) concept.** VRM = Versatile Remediation Module. *Note: This is an early concept for illustration purposes and is subject to change.*

## II. Versatile Remediation Module Design Description

The design of the VRM was driven by the canister configuration (i.e., cylindrical wall with nominal diameters in the range of 1701.8 to 1917.7 mm (67 to 75.5 in.) and anticipated environment (i.e., radiation and temperature levels). Gamma dose rate was conservatively estimated at 5 kRad/hr. Temperature was assumed to be less than 100°C. The VRM main configuration and components are shown in Figs. 3 to 5. The main equipment that makes up the VRM includes (1) the support base, (2) the radial carriage and actuator, (3) the welding head, (4) the welding head base and axial actuator, (5) the fume extraction box, (6) the instrumentation and control (i.e., sensors, motor drives, and controllers necessary for control of the VRM), and (7) operating workstation with a graphical user interface (GUI) displayed on a monitor and controlled by a joystick, keyboard, and mouse.

The VRM consists of a gas tungsten arc welding (GTAW) torch to perform the required repair welds. Cold-wire GTAW (CW-GTAW) was selected primarily for its ability to provide high-quality welds with optimum control of the welding variables. Additionally, CW-GTAW is applicable to both 304/304L and 316 steels (i.e., common confinement materials), and significant prior experience exists in using CW-GTAW automated welding for critical applications in nuclear and piping industries (i.e., historic reliability). The weld torch is rated for 150 amps at 60% duty cycle and is air cooled to eliminate the possibility of cooling water accidentally being released near the canister, which could cause a criticality or corrosion concern. For repair welding operations, the VRM can apply parallel linear weld beads in a singular direction spaced apart by half the diameter of the weld bead (filler rod must lead the welding arc). During welding operations, the arc gap is dynamically controlled through Arc Voltage Control (AVC) software, which constantly measures the voltage across the arc and makes slight adjustments to the standoff distance to maintain the preprogrammed voltage. A wire feeder assembly provides and guides weld filler wire to the arc in front of the tungsten electrode. Ultra-high-purity argon gas is used as a cover gas to reduce unwanted chemical reactions and contaminants in the weld. The repair space to perform a repair weld is an approximately 15 x 15 cm (6 × 6 in.) square.

The VRM achieves coordinated motion through three modes of actuation (radial, vertical, and angular). All modes of actuation are protected by mechanical stops and limit switches. For the radial actuation, an ultrasound proximeter is used to determine the initial standoff from the canister. Once the weld torch is within an inch of the canister, the torch provides additional standoff information. The welding module allows for radial actuation of at least 20 cm (8 in.) to accommodate canisters of smaller diameters. Motors used for the module are alternating current (AC) servo motors with drivers capable of moving the respective parts of the module at up to 12 mm/s (0.5 in./s). AC synchronous servo motors with onboard resolvers and AC drivers are the most advantageous for this application because they will not require additional sensors to provide positioning information to the control system. Resolvers were chosen over optical encoders because of their superior radiation resistance. Optical encoders include glass discs that darken with radiation exposure; after higher levels of radiation exposure, the disk will become too dark to determine position. Another downfall of the optical encoders is that they use photodiodes to detect light from an LED. The photodiodes typically produce signals on the order of 5 volts. This low voltage would not be able to be read at very far distances, thus requiring radiation-sensitive electronics close to the motor. Two onboard radiation tolerant cameras are mounted to allow for direct viewing of the front and back of the weld. To allow active weld viewing, a solenoid-actuated shutter is used to move weld glass in front of the camera lenses during the time that the arc is struck.

The VRM is not designed for remote maintenance. Given that repairs are not expected to last long, the VRM is designed for maintenance in between repairs and when removed away from the radioactive boundary. However, the VRM is designed to be robust with analog components and redundant radiation resistant cameras, so periodic maintenance is not expected to be frequent. Further, all components are

off-the-self to minimize costs and facilitate replacement, if needed. Decommissioning would involve disassembling the VRM and segmenting the components to reduce volume. The VRM is not expected to be surface contaminated or activated. The VRM exterior surface is designed to be smooth to facilitate decontamination. In the unlikely event that contamination is found on the VRM surface, the MERF could be decommissioned following decontamination and segmentation. It could then be disposed as low-level waste in accordance with the appropriate regulatory requirements.

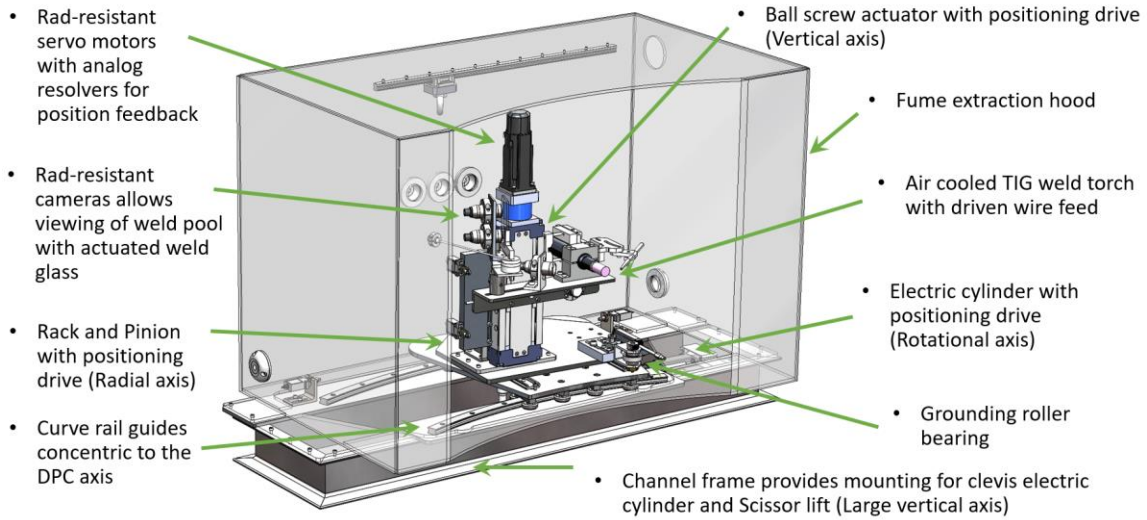


**Figure 3. Main VRM configuration and components.** *Note: the fume extraction hood is to protect personnel working on the development of VRM. This system will not be part of the final MERF.*

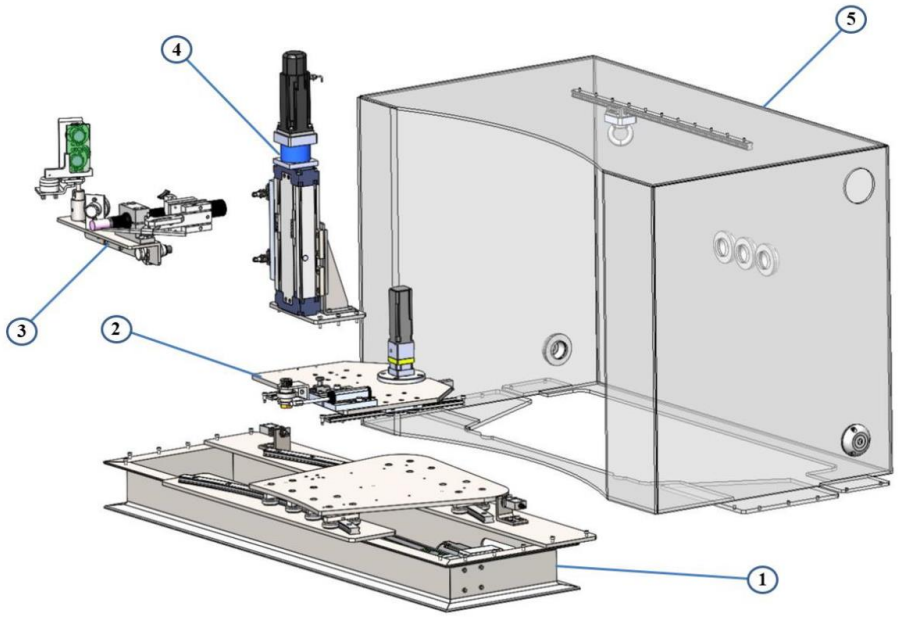


**Figure 4. VRM exploded view.** (1) Support base; (2) Radial carriage and actuator; (3) Welding head; (4) Welding head base and axial actuator; (5) Fume extraction box.

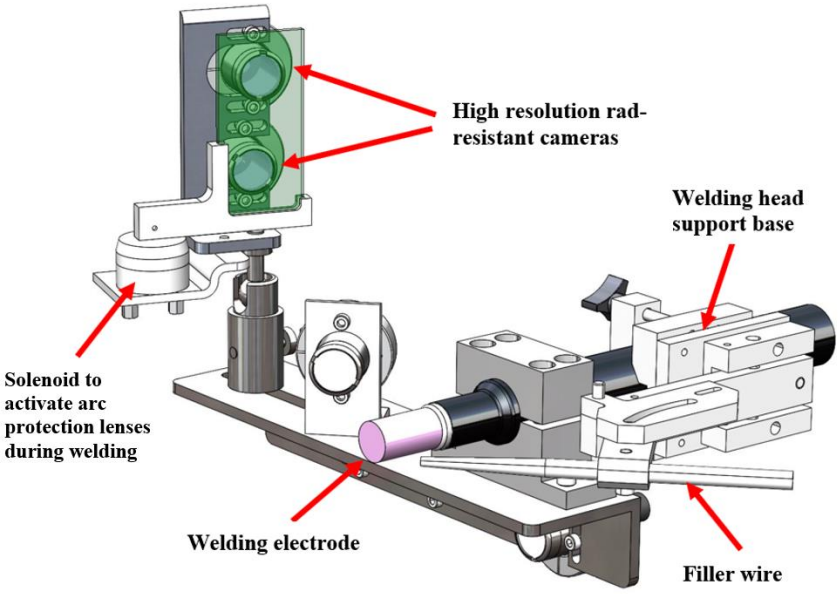


**Figure 5. Welding head details.**

### III. Control System

The VRM remote control system has two levels: The first level comprises software modules that allow the operator to remotely supervise, manage, and control the VRM from a workstation, (e.g., positioning equipment, initiating weld-related operations). The second level comprises hardware modules, which include motor controllers, position controllers, automated welding controllers, switches, and more. The VRM control system takes positioning information from the three motor resolvers on the module and ultrasound proximeter to provide the system with position information of the weld torch. Using that position information, the control system initiates a preprogrammed welding sequence at the proper time to provide enough gas purge time, strike an arc, and initiate the weld wire feed roller to start the weld bead at the proper location. The control system is broken down to individual components with a central controller coordinating the devices and the remote operators. Figure 6 provides an example architecture of the control system.

A real-time controller is used to integrate all the process controls into a cohesive architecture, switch on/off, and provide data acquisition from sensors, weld power supply control, weld torch control (via AVC), video input from cameras, and motion control of all motors. The real-time controller interfaces directly with the operator workstation to display data and control information to operators by using standard ethernet communication, which allows for remotely locating the operator workstation computer. This interface is an ideal architecture for operating equipment in a hazardous environment since the real-time controller can be located near the VRM, minimizing the cable lengths needed to control the hardware, whereas the operation workstation can be in a safe area to minimize hazards to the operator.

The operator workstation has a GUI that is displayed on a monitor and controlled with a combination of a joystick, keyboard, and mouse. This workstation provides the operator with a level of familiarity to the computer system to reduce training needs. The operator video monitors interface with the cameras. The operator workstation includes video and data recording capabilities for the recording and playback of operations in the event of off-normal conditions that need further analysis, and as a permanent record

of the processes performed. Finally, there is the capability for an “operator manual override” designed into the system and joysticks for manual control of all motors.

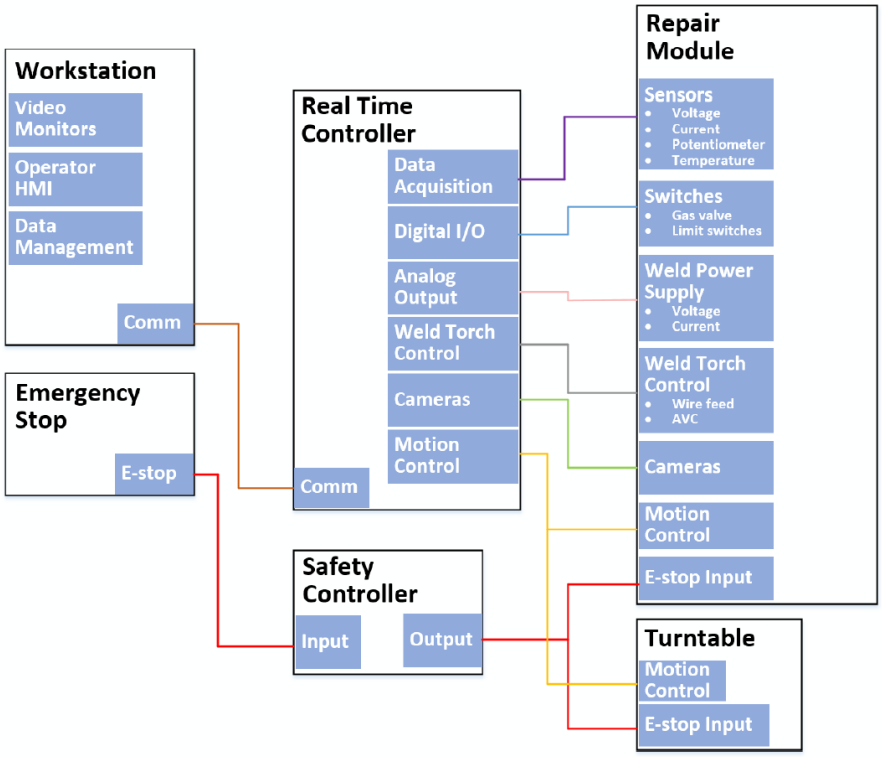


**Figure 6. Control system architecture.** The top-level components for the purpose of control are the (1) real time controller, (2) operating workstation, (3) repair module, (4) turntable, (5) safety controller, and (6) hardware emergency stop.

The safety controller is the primary safety control that prevents and inhibits operations that could have significant safety implications. The safety controller is independent of the real-time controller and operator workstation and operates on independent inputs and outputs, which prevents any interference between the controls systems. The emergency stop (e-stop) system is integrated with the safety controller and provides inputs that the operator can use to shut down the system in the event of off-normal conditions that could have safety implications. This e-stop system consists of mushroom type e-stop switches located at the operator workstation. An important consideration of the e-stop system is that motion cannot be automatically re-initiated upon clearing of the e-stop switches. Motion can only be re-initiated upon command by the operator after the e-stop condition has been cleared.

### IV. Equipment Layout

The VRM prototype is assembled in the “pit” of Building 7603 at ORNL and is operated remotely from the adjacent mezzanine (Fig. 7). The operator workstation is in the mezzanine with no direct line of sight to the pit. The motion and controls equipment are housed in a control cabinet adjacent to the operator workstation. Cable length between the VRM and operator workstation is approximately 40 m (120 ft). This layout simulates the remote location of the electronics from the field radiative environment. Additional equipment installed in the pit area includes a welding machine, cover gas cylinders, a rotating table (turntable), a full-scale mockup canister, a fume exhaust system for removing fumes generated during the repair process, and a scissor lift that supports and positions the VRM at the height of the area

where repair will take place. The as-built equipment configuration during the development and demonstration phase is shown in Fig. 8.

The rotating table allows the canister to rotate in clockwise and counterclockwise directions and is needed to position the canister to present the flaw/defect area in front of the VRM. The rotating table consists of three main components: a table, a bearing/drive, and a support structure. The table is constructed out of powder-coated, 3.81 cm (1.5 in.) thick A36 carbon steel with a hole in the center. It is designed for rigidity as opposed to strength and thus can support the canister without any sizable deflection. The slewing ring bearing is rated for 136,000 kg (300,000 lb) under static loading conditions and 36,287 kg (80,000 lb) in dynamic loading conditions. The support structure is constructed out of steel structural beams. Its main purpose is to distribute the load from the rotating table over a larger area. With the use of the support structure, the rotating table is floor-limited at 8,164 kg (18,000 lb). For seismic considerations, 42 cm (16¾ in.) bolts are used to mount the rotating table to the floor.

A full-scale welded 304/304L mockup canister using the same materials and fabrication as a real canister was manufactured for testing and demonstration of the VRM. Currently, nearly all storage canister designs use 304 or 304/304L stainless steel and are constructed predominantly using multi-pass arc welding with a double-V edge preparation. The mockup canister comprises two cylindrical shells, each 1819.2 mm (71.625 in.) long and 1828.8 mm (72 in.) in diameter. With the addition of the 19.05 mm (0.75 in.) thick bottom plate, the mockup canister is 3657.6 mm (144 in.) high, 1828.8 mm (72 in.) in diameter, and 12.7 mm (0.5 in.) thick. The canister has two longitudinal welds and one circumferential weld to join the two cylindrical shells. Another circumferential weld joins the canister shell with the bottom plate. Each shell was formed by cold forming a plate into a cylinder and then making a single longitudinal weld to form the cylinder. Each weld was subjected to visual and dye penetrant inspections.

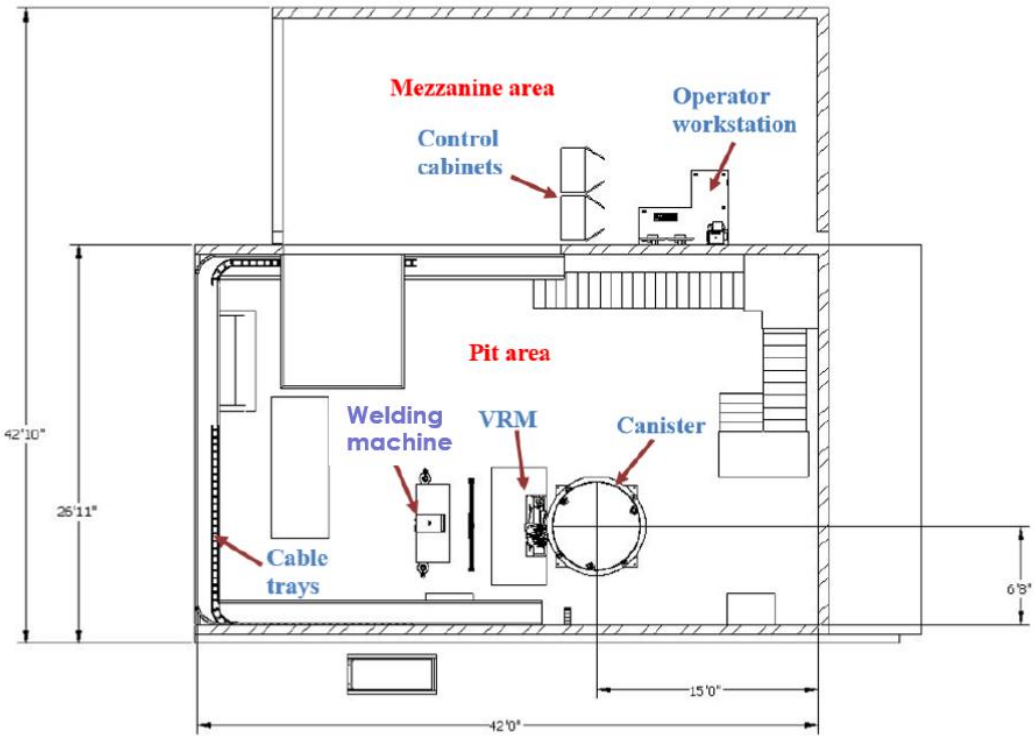


**Figure 7. Equipment layout (dimensions are in inches).** This layout simulates the remote location of the electronics from the field radiative environment. All development tasks occur in this non-radiation environment of the test area. VRM = Versatile Remediation Module.

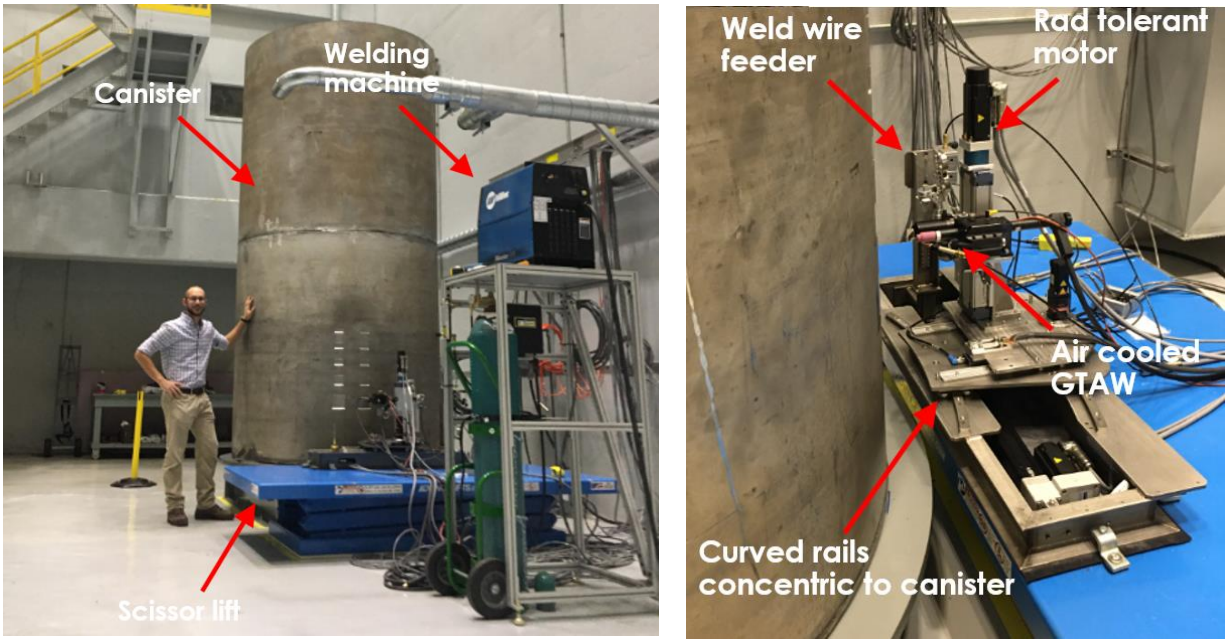


**Figure 8. "As-built" equipment configuration during development and demonstration phase.** Left: as-built equipment configuration during development and demonstration phase. Right: a full-scale welded 304/304L mockup canister using the same materials and fabrication methods as a real canister with embedded flaws to evaluate and demonstrate the Versatile Remediation Module.

## V. Demonstration and Results

### V.A Weld Trials for Parameter Selection

CW-GTAW trials were performed on 304/304L stainless steel plates with simulated shallow and deep or through-thickness cracks to select proper welding parameters, including welding current, voltage (arc gap), wire feed speed, and welding travel speed. To simulate shallow cracks, eight artificial cracks with 3.175 mm (⅛ in.) depths were produced by a milling machine on two pieces of 12.7 mm (0.5 in.) thick 304L stainless steel plate. To simulate deep or through-thickness defects, waterjet cutting was used to create three 38.1 mm (1.5 in.) long through-thickness artificial cracks on a 12.7 mm (0.5 in.) thick 304L stainless steel plate. A hand grinder was used to produce simulated crack excavations. Shallow cracks were excavated by the hand grinder. For deep cracks, two kinds of excavations were performed: one 3 mm (~⅛ in.) deep, and the other 9.5 mm (~⅜ in.) deep. Shallow (3 mm) and deep (9.5 mm) grooves were made to simulate partial penetration repair welding and full penetration repair welding, respectively. Argon cover gas (100%) was used for shallow crack repair welding, and 75% He + 25% Ar shielding was used for deep crack repair welding. Two CW-GTAW welding passes were applied on the shallow excavations, and six on the deep excavations. All weld trials passed the visual and liquid penetrant evaluations. Welding parameters that resulted in adequate penetration without observable defects were selected for qualification and demonstration. The selected welding parameters are shown in Table 1.

Table 1. CW-GTAW parameters selected for qualification [17].

| Welding process | Current (A) | Travel speed (cm/min) | Wire feed speed (cm/min) |
|---|---|---|---|
| CW-GTAW | 135 | 10 | 50.8 |

### V.B Weld Procedure Qualification

The weld repair procedure qualification was carried out with 9.52 mm (3/8 in.) certified 304/304L stainless steel plates. Two welds were produced for procedure qualifications: one with 100% Ar cover gas and the second with 75% He + 25% Ar cover gas to improve the welding penetration. Visual inspection of the welds on 9.52 mm (⅜ in.) test plates was acceptable. Face and root weld transverse side-bend tests were carried out on GTAW welds and were acceptable to the requirements of the ASME Boiler and Pressure Vessel Code [17]. Transverse tensile tests were also performed and met the requirements of the ASME Boiler and Pressure Vessel Code, the results of which are shown on the right side of Fig. 9. Yield strength was 294 MPa. Ultimate tensile strength was 627 MPa, which is higher than that required by the ASME Boiler and Pressure Vessel Code (482 MPa) [18].

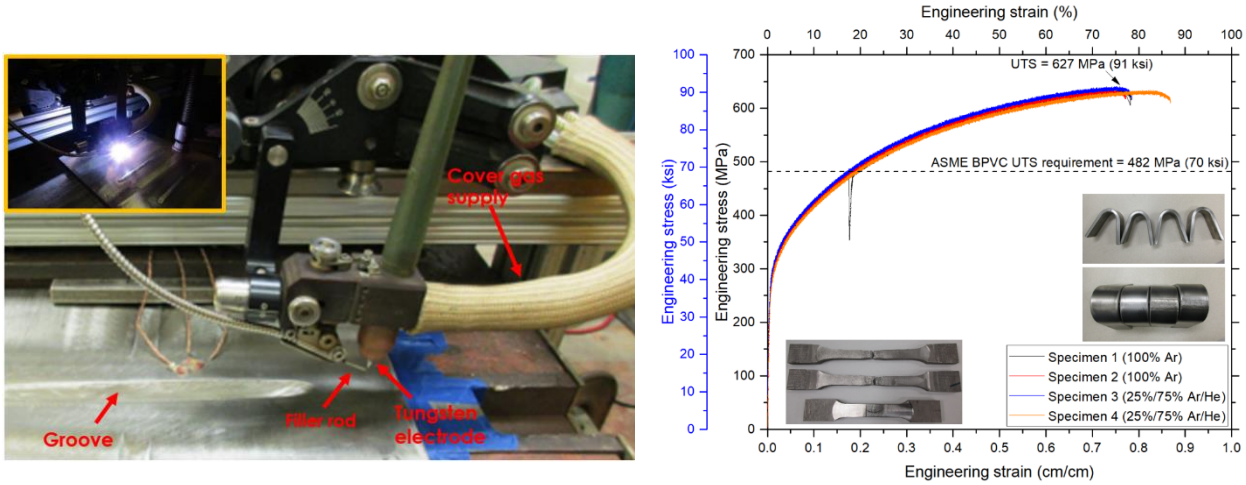


**Figure 9. Welding configuration and qualification tensile and bend test results. Left:** Left: welding configuration; gas tungsten arc welding (CW-GTAW) torch used for performing a weld repair. The electrode was tungsten, the filler rod was 308L stainless steel, and the cover gas was mixture of 75% He + 25% Ar. Right: CW-GTAW joint transverse tensile curves and bend tests for different cover gases.

### V.C Operational sequence

A typical operational procedure consists of the following steps. First, the operator, using the motion control system, positions the welding torch over the start of the area to be welded. The operator visually verifies torch location using the welding cameras. Following a touch-retract torch movement to position the torch at a proper standoff location, the shield cover gas is turned on and run for a specific period of time (typically 5–10 s) to purge air in the vicinity of the weld. After the gas purge, weld power supply is enabled and an open circuit voltage is measured to verify the power supply is operating properly. After verification that the power supply is enabled, the welding arc is initiated via touch start (in this case, the torch is moved until light contact is made with the base material, and then lifted to initiate the arc) or high-frequency start. Care must be taken that the tungsten torch is not pushed too hard into the material, to prevent tungsten breakage or tungsten contamination of the base metal. After arc start, the torch is moved via the preprogrammed path while maintaining the proper voltage via the

AVC. As the welding progresses, the operator observes the process in the arc viewing cameras and can make adjustments to the welding process as needed. These adjustments are typically lateral position of the torch to ensure good wetting of the groove sidewalls, and position of the weld wire in the weld pool to ensure good wire melting. GTAW welding speeds are typically 5–15 cm (2–6 in.) per minute, which is relatively slow. These slow speeds allow time for the operator to make these adjustments without an overwhelming workload. Experience showed that adjustments are typically necessary only during the first inch or so of welding.

**V.D. Neutron diffraction residual stress measurements before and after repair**

Neutron diffraction was performed at the Neutron Residual Stress Mapping Facility (NRSF2) of the High Flux Isotope Reactor at ORNL to assess the residual stress profiles before and after a weld repair [19-21]. The NRSF2 exploits the large penetration depth of neutrons to measure residual stresses deep within a material by detecting the change in the diffraction pattern of an incident neutron beam. Neutron diffraction is the only nondestructive method that can provide a through-thickness mapping of residual stress in steel. Residual strains in x (longitudinal/axial—welding direction), y (transverse/hoop), and z (normal/radial) directions along the five contours were measured. The measured strains in the radial direction were near zero. Thus, the plane strain condition was justified to calculate the weldment strain and stress accordingly in the hoop and axial directions. The details of the test results for the hoop (circumferential), radial, and axial (longitudinal) residual stresses profiles for as-welded and repaired specimens are shown in Fig. 10. The maximum tensile residual stress for the as-welded specimen was 340 MPa. The maximum residual stress was in the fusion zone and oriented in the axial direction. The residual axial tensile stress also indicates that tensile stresses exist throughout the thickness of the weldment in the fusion zone. For the repaired specimen, the maximum axial tensile residual stress increased by ~65 MPa to 406 MPa (from 340 MPa on the as-welded specimen), and there was a shift in position. However, the full profile was not tensile through-thickness, and there were regions where compressive stresses have been introduced. Similarly, for the repaired hoop, residual stresses significantly reduced compared with the as-welded residual stresses. This reduction indicates that the repair could redistribute the stresses in a beneficial way. Note that the specimen was constrained during repair to simulate a representative field repair, but the specimen had to be released during neutron diffraction measurements. As a result, there may have been some additional stress relaxation when the constraint was released that has not been accounted for during the neutron diffraction measurements.

**V.E Procedure demonstration**

A complete remote repair weld was demonstrated on a “pocket” excavated on the canister surface. The pocket was completely filled with welding material using the VRM that was preprogrammed to perform the operation fully automated. The pocket was filled with 5 weld passes in ~10 min. Similar welding parameters that were used during the repair welding procedure qualification were used for the repair welding demonstration. The completed repair weld is shown in Fig. 11.

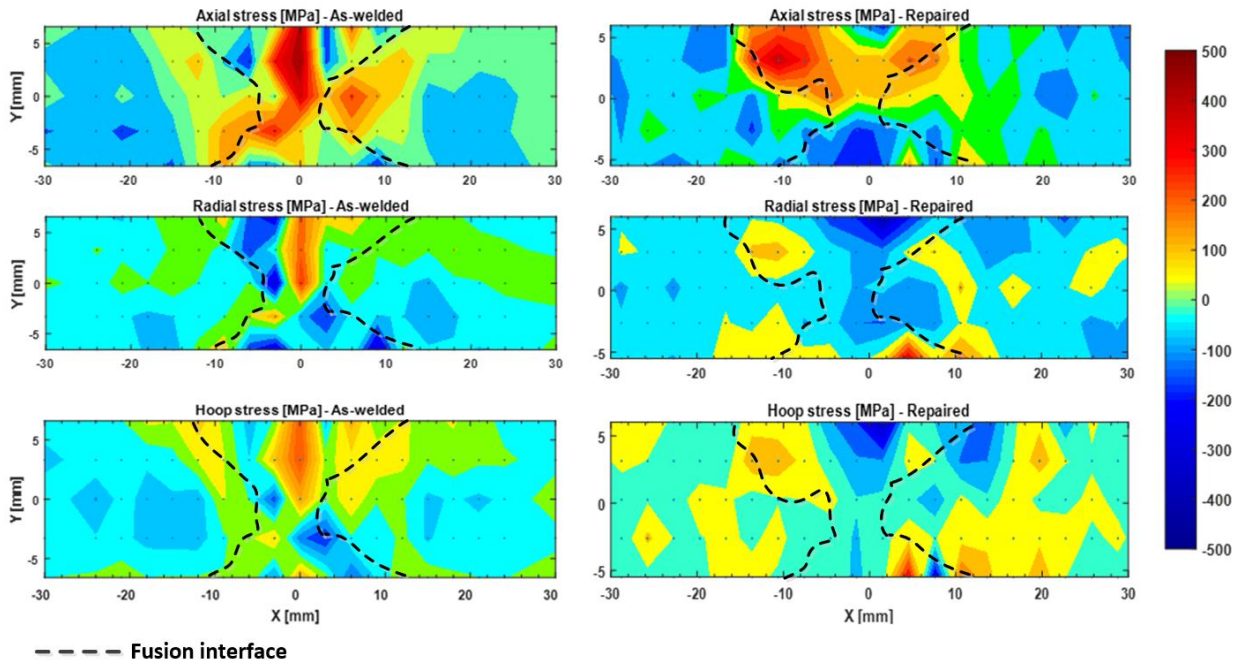


**Figure 10. Through-thickness residual stress contour mapping for as-welded and repaired specimen.** Axial, radial, and hoop residual stress through-thickness mapping for as-welded (left column) and repaired (right column) specimen. The dotted line represents the fusion zone interface. High tensile residual stresses are observed throughout the thickness of the as-welded specimen in the fusion zone and heat-affected zone (HAZ). A redistribution in residual stresses is observed in the repaired specimen.

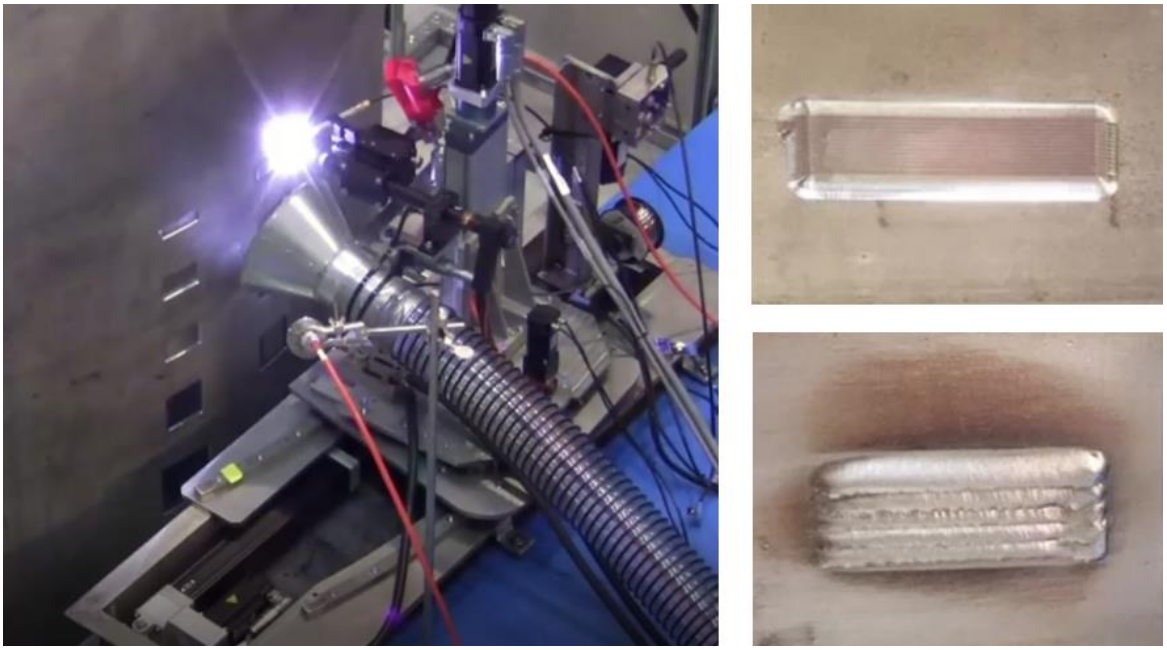

**Figure 11. VRM in operation and completed repair weld.** Left: snapshot of VRM in operation. Top right: as-excavated "pocket" on canister surface. Bottom right: pocket filled with 5 passes of overlay weld material.

**Acknowledgements**

This material is based upon work supported by the US Department of Energy, Office of Nuclear Energy, under contract number DE-AC05-00OR22725. The authors would like to thank John Kessler, Brian Gutherman and Adam Levin for expert input and guidance during the initial concept development, Paris Cornwell for his technical assistance in the neutron diffraction experiments, Craig Mauer and Christopher Crawford for technical support in the design, and Doug Kyle who performed the repair welding.

**Disclaimer**

This is a technical paper that does not take into account contractual limitations or obligations under the Standard Contract for Disposal of Spent Nuclear Fuel and/or High-Level Radioactive Waste (Standard Contract) (10 CFR Part 961). For example, under the provisions of the Standard Contract, spent nuclear fuel in multi-assembly canisters is not an acceptable waste form, absent a mutually agreed to contract amendment.

To the extent discussions or recommendations in this paper conflict with the provisions of the Standard Contract, the Standard Contract governs the obligations of the parties, and this presentation in no manner supersedes, overrides, or amends the Standard Contract.

This paper reflects technical work which could support future decision making by DOE. No inferences should be drawn from this presentation regarding future actions by DOE, which are limited both by the terms of the Standard Contract and a lack of Congressional appropriations for the Department to fulfill its obligations under the Nuclear Waste Policy Act including licensing and construction of a spent nuclear fuel repository.

**Competing Interests**

The authors declare no competing interests.

**Data Availability**

The raw/processed data required to reproduce these findings cannot be shared at this time due to technical or time limitations. However, the raw/processed data required to reproduce these findings will be made available online during the review process and prior to publication.

**References**

1. Yi, X., Jinsuo, Z. Chloride-induced stress corrosion cracking of used nuclear fuel welded stainless steel canisters: A review. *J Nuc Mater*, 466, 85-93, 2015.

2. Cattant, F., et al. Corrosion issues in nuclear industry today. *Materials Today*, **11**(10), 32-37, 2008.

3. Electric Power Research Institute (2017). Aging Management Guidance to Address Potential Chloride-Induced Stress Corrosion Cracking of Welded Stainless Steel Canisters. Report no. 300200819. Palo Alto, CA.

4. United States Nuclear Regulatory Commission (2010). Atmospheric Stress Corrosion Cracking Susceptibility of Welded and Unwelded 304,304L, and 316L Austenitic Stainless Steels Commonly Used for Dry Cask Storage Containers Exposed to Marine Environments. NUREG/CR-7030.

5. United States Nuclear Regulatory Commission (2012). Potential Chloride-Induced Stress Corrosion Cracking of Austenitic Stainless Steel and Maintenance of Dry Cask Storage System Canisters. NRC Information Notice 2012-20, 2012.

6. Electric Power Research Institute (2015). Susceptibility assessment criteria for chloride-induced stress corrosion cracking (CISCC) of welded stainless steel canisters for dry cask storage systems. Report no. 3002005371. Palo Alto, CA.

7. United States Nuclear Regulatory Commission (2011). Materials Aging Issues and Aging Management for Extended Storage and Transportation of Spent Nuclear Fuel. NUREG/CR-7116.

8. Nuclear Energy Institute (2019). Sixth Update to the Industry's Research and Development Priorities Specific to the Long-Term Dry Storage and Transportation of Used Nuclear Fuel. Letter to U.S. Department of Energy.

9. S. Chatzidakis et al. (2019). System-Wide Impacts of Resolution Options for a Nonconforming Dry Storage System. Proceedings of the 2019 Global/TopFuel conference, pp. 1040-1047, Seattle, WA.

10. S. Chatzidakis et al. (2018). A Novel Mobile Examination and Remediation Facility for On-Site Remediation of Dry Storage Systems. Proceedings of the Waste Management Conference, March 18-22, Phoenix, AZ.

11. United States Department of Energy (2015). *Dry Storage Cask Inventory Assessment*. Prepared for DOE, Nuclear Fuels Storage and Transportation Planning Project, Jones Jr., Robert H. (Savannah River National Laboratory). Report no. FCRD-NFST-2014-000602, Revision 1.

12. United States Nuclear Regulatory Commission (2013). Finite Element Analysis of Weld Residual Stresses in Austenitic Stainless Steel Dry Cask Storage System Canisters. Technical Letter Report, 2013.

13. United States Nuclear Regulatory Commission (2014). Identification and Prioritization of the Technical Information Needs Affecting Potential Regulation of Extended Storage and Transportation of Spent Nuclear Fuel, May 2014.

14. United States Nuclear Waste Technical Review Board (2010). Evaluation of the Technical Basis for Extended Dry Storage and Transportation of Used Nuclear Fuel.

15. Pacific Northwest National Laboratory (2015). Gap Analysis to Support Extended Storage of Used Nuclear Fuel. Hanson, B., H. Alsaed, C. Stockman, D. Enos, R. Meyer, and K. Sorenson. Used Fuel Disposition Campaign, Revision 0, 2015.

16. Argonne National Laboratory (2014). Managing Aging Effects on Dry Cask Storage Systems for Extended Long-Term Storage and Transportation of Used Fuel. Report no. ANL-13/15, Revision 2, September 2014.

17. Tang, W., et al. (2019). Welding process development for spent nuclear fuel canister repair. Proceedings of the ASME-PVP2019, July 14–19, San Antonio, TX.

18. ASME Boiler and Pressure Vessel Code, 2017 Edition.

19. Cornwell, P., et al. Current capabilities of the residual stress diffractometer at the High Flux Isotope Reactor. *Review of Scientific Instruments*, **89**(9), 092804 (2018). doi:10.1063/1.5037593.

20. S. Chatzidakis, et al. (2019). *Neutron Residual Stress Mapping of Repaired Spent Nuclear Fuel Welded Stainless-Steel Canisters*. Proceedings of the International Conference on High-Level and Radioactive Waste Management (IHLRWM 2019), April 14-18, Knoxville, TN.
21. S. Chatzidakis, et al. (2019). *Neutron Diffraction Illustrates Residual Stress Behavior of Welded Alloys Used as Radioactive Confinement Boundary*. International Journal of Pressure Vessel and Piping, under review.